9. Johannessen, T., Jansen, E., Flatøy, A. & Ravelo, A. C. in *Carbon Cycling in the Glacial Ocean: Constraints on the Ocean's Role in Global Change* (eds Zahn, R. *et al.*) 61–85 (Springer, Berlin, 1994).
10. Gard, G. & Backmann, J. in *Geological History of the Polar Oceans: Arctic Versus Antarctic* (eds Bleil, U. & Thiede, J.) 417–436 (Kluwer, Dordrecht, 1990).
11. Gard, G. *Paleoceanography* **2,** 519–529 (1987).
12. Baumann, M. in *Geological History of the Polar Oceans: Arctic versus Antarctic* (eds Bleil, U. & Thiede, J.) 437–445 (Kluwer, Dordrecht, 1990).
13. Carstens, J. & Wefer, G. *Mar. Micropaleont.* (submitted).
14. Emerson, S. & Hedges, J. I. *Paleoceanography* **3,** 621–634 (1988).
15. Hebbeln, D. *Boreas* **21,** 295–304 (1992).
16. Wagner, T. *Ber. Sonderforschungsber. 313, Univ. Kiel* **42,** (1993).
17. Wagner, T. & Henrich, R. *Mar. Geol.* (in the press).
18. Spielhagen, R. F. *GEOMAR-Report* **4,** (1991).
19. Imbrie, J. & Kipp, N. G. in *The Late Cenozoic Glacial Ages* (ed. Turekian, K. K.) 71–181 (Yale Univ. Press, 1971).
20. Kellogg, T. B. *Paleoceanography* **2,** 259–271 (1987).
21. Bischof, J. in *Geological History of the Polar Oceans: Arctic versus Antarctic* (eds Bleil, U. & Thiede, J.) 499–518 (Kluwer, Dordrecht, 1990).
22. Henrich, R. in *Geological History of the Polar Oceans: Arctic versus Antarctic* (eds Bleil, U. & Thiede, J.) 213–244 (Kluwer, Dordrecht, 1990).
23. Hancock, J. M. in *Introduction to the Petroleum Geology of the North Sea* (ed. Glennie, K. W.) 133–150 (Blackwell, Oxford, 1984).
24. Elverhøi, A. *Norsk geol. Tidsskr.* **59,** 273–284 (1979).
25. Mangerud, J. in *Klimageschichtliche Probleme der letzten 130.000 Jahre* (ed. Frenzel, B.) 307–330 (Fischer, Stuttgart, 1991).
26. Lehmann, S. J. *et al. Nature* **349,** 513–516 (1991).
27. Sigmond, E. M. O. *Bedrock Map of Norway and adjacent Ocean Areas. Scale 1:3 Million* (Geol. Surv. of Norway, Oslo, 1991).
28. Vorren, T. O., Vorren, K.-D., Alm, T., Gulliksen, S. & Løvlie, R. *Boreas* **17,** 41–77 (1988).
29. Johnsen, S. J., Dansgaard, W. & White, J. W. C. *Tellus* **41B,** 452–468 (1989).
30. Heinrich, H. *Quat. Res.* **29,** 142–152 (1988).
31. Bond, G. *et al. Nature* **360,** 245–249 (1992).
32. Grousset, F. E. *et al. Paleoceanography* **8,** 175–192 (1993).
33. Hughes, T. J. *Boreas* **16,** 89–100 (1987).
34. Johannessen, O. M. in *The Nordic Seas* (ed. Hurdle, B. G.) 103–127 (Springer, New York, 1986).
35. Mangerud, J. & Gulliksen, S. *Quat. Res.* **5,** 263–273 (1975).
36. Kellogg, T. B. *Can. J. Earth Sci.* **21,** 189–193 (1984).
37. Carstens, J. & Wefer, G. *Deep-Sea Res.* **39,** suppl. 2, S507–S524 (1992).
38. Bard, E., Arnold, M., Fairbanks, R. & Hamelin, B. *Radiocarbon* **35,** 191–199 (1993).

ACKNOWLEDGEMENTS. Core NP90-39 was collected in 1990 by the RV *Hakon Mosby* (Norwegian Polar Research Institute); the other cores were taken from the RV *Polarstern* expedition ARK III/3. We thank E. Jansen and R. Søraas for measuring stable isotopes on core NP90-39, G. Bonani for conducting AMS-analyses on cores 1294-4 and 1295-5, and W. H. Berger for reading the manuscript. D.H. was supported by the Bundesministerium für Forschung und Technologie and T.D. by the Norwegian Research Council and the Norwegian Polar Research Center.

Decade-scale trans-Pacific propagation and warming effects of an El Niño anomaly

G. A. Jacobs*, H. E. Hurlburt*, J. C. Kindle*, E. J. Metzger*, J. L. Mitchell*†, W. J. Teague* & A. J. Wallcraft‡

* Naval Research Laboratory, Stennis Space Center, Mississippi 39529, USA
† Colorado Center for Astrodynamics Research, University of Colorado, Boulder, Colorado 80303, USA
‡ Planning Systems Incorporated, Stennis Space Center, Mississippi 39529, USA

El Niño events in the Pacific Ocean can have significant local effects lasting up to two years. For example the 1982–83 El Niño caused increases in the sea-surface height and temperature at the coasts of Ecuador and Peru[1], with important consequences for fish populations[2,3] and local rainfall[4]. But it has been believed that the long-range effects of El Niño events are restricted to changes transmitted through the atmosphere, for example causing precipitation anomalies over the Sahel[5]. Here we present evidence from modelling and observations that planetary-scale oceanic waves, generated by reflection of equatorial shallow-water waves from the American coasts during the 1982–83 El Niño, have crossed the North Pacific and a decade later caused northward re-routing of the Kuroshio Extension—a strong current that normally advects large amounts of heat from the southern coast of Japan eastwards into the mid-latitude Pacific. This has led to significant increases in sea surface temperature at high latitudes in the northwestern Pacific, of the same amplitude and with the same spatial extent as those seen in the tropics during important El Niño events. These changes may have influenced weather patterns over the North American continent during the past decade, and demonstrate that the oceanic effects of El Niño events can be extremely long-lived.

The observational evidence for this re-routing of a portion of the Kuroshio Extension comes from satellite altimeter and infrared data. Significant changes in sea surface height (SSH) are seen in a combined analysis of altimeter data from the Geosat-Exact Repeat Mission satellite (Geosat-ERM)[6] and the European Remote Sensing satellite (ERS-1). The resulting change in SSH (Fig. 1*a*) represents a change in ocean circulation over the interval from 1988 to 1993. Similar results are obtained by a combination of TOPEX/POSEIDON (a joint USA NASA/French CNES altimeter satellite) and Geostat-ERM altimeter data.

FIG. 1 *a*, Latitude–longitude plot showing change in sea surface height (SSH) from the Geosat-ERM (November 1986 to October 1989) to ERS-1 (April 1992 to March 1993) observations. The colour bar at the bottom of the Figure indicates changes from −15 to 15 cm. The long time period average position of the Kuroshio Extension[17] is plotted so that the positions of the features may be compared. Large-scale circulation in the oceans is approximated by the geostrophic relation, which implies that water flows along lines of constant height with higher SSH to the right when facing downstream. Thus changes in SSH are related to changes in ocean circulation. The high SSH anomaly north of the Kuroshio Extension at 175° E indicates a northward shift of a portion of the Kuroshio Extension's transport. *b*, Deviation of sea surface temperature (SST) averaged over April 1992 to March 1993 from a mean over 1985–92. Data were supplied by infrared radiometer satellites[7]. The colour bar indicates anomalies from −1 to 1 °C. The high SST anomaly extending eastwards from Japan at ~40° N is just north of the SSH anomaly in *a*, as would be expected by the circulation changes implied by *a*. *c*, Change in model SSH from the time of the Geosat-ERM (November 1986 to October 1989) to the ERS-1 time frame (April 1992 to March 1993). These are the same time periods as covered by the altimeter satellites in *a*. A ridge of SSH extends from Japan to the Gulf of Alaska. *c* is provided by a six-layer, 0.25°-resolution, primitive equation ocean model[18–20] of the global ocean circulation. This model is based on conservation of momentum and mass and has current velocity, ocean pressure and SSH as variables. The boundary follows the 200-m isobath. This simulation is forced only by winds, and is spun up to statistical equilibrium by forcing with the Hellerman and Rosenstein wind stress climatology[21]. Subsequently, the model is forced from 1981 to 1993 with daily 1,000 mb winds derived from the European Centre for Medium-Range Weather Forecasts with the annual mean replaced by that of Hellerman and Rosenstein[20]. The model reproduces all of the major current systems of the North Pacific including the equatorial currents and the Kuroshio Extension[20].

In Fig. 1*a*, a positive SSH anomaly centred just south of 40° N at 175° E lies north of the Kuroshio Extension. The anomaly indicates that a portion of the current is re-routed to a path that follows the northern slope of the anomaly. The circulation changes imply changes in sea surface temperature (SST) as warm waters are advected further north. A consistent set of global SSTs has been compiled since 1985 by Reynolds[7]. A warm SST anomaly north of the Kuroshio Extension is clearly seen in Fig. 1*b*, extending from Japan to North America at 40° N. This SST anomaly is just north of the SSH anomaly as expected (Fig. 1). Thus, both satellite-sensed SSH and SST strongly suggest a northward shift of a portion of the Kuroshio Extension, and a subsequent anomalous northward transport of warm waters.

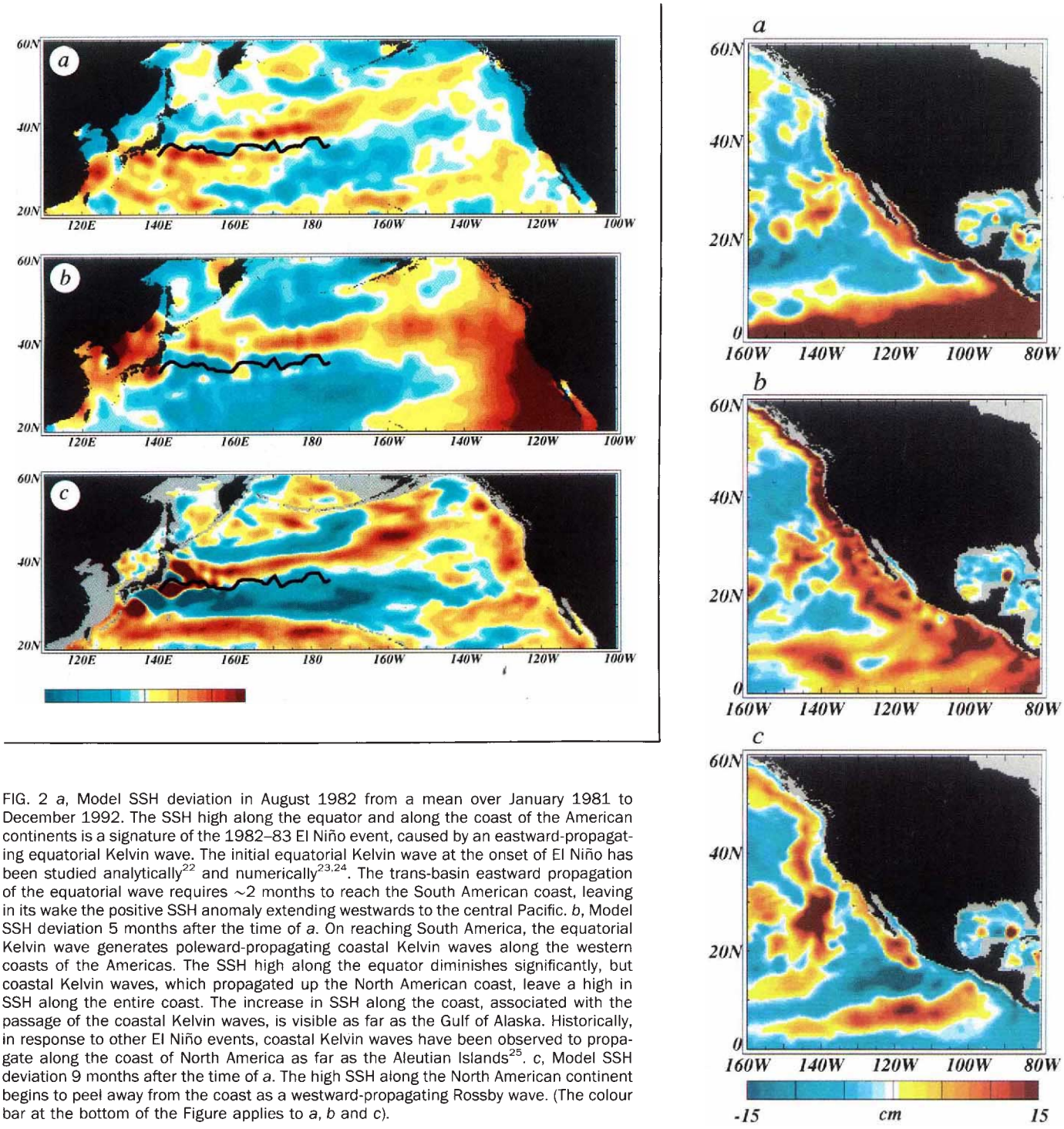

FIG. 2 *a*, Model SSH deviation in August 1982 from a mean over January 1981 to December 1992. The SSH high along the equator and along the coast of the American continents is a signature of the 1982–83 El Niño event, caused by an eastward-propagating equatorial Kelvin wave. The initial equatorial Kelvin wave at the onset of El Niño has been studied analytically[22] and numerically[23,24]. The trans-basin eastward propagation of the equatorial wave requires ~2 months to reach the South American coast, leaving in its wake the positive SSH anomaly extending westwards to the central Pacific. *b*, Model SSH deviation 5 months after the time of *a*. On reaching South America, the equatorial Kelvin wave generates poleward-propagating coastal Kelvin waves along the western coasts of the Americas. The SSH high along the equator diminishes significantly, but coastal Kelvin waves, which propagated up the North American coast, leave a high in SSH along the entire coast. The increase in SSH along the coast, associated with the passage of the coastal Kelvin waves, is visible as far as the Gulf of Alaska. Historically, in response to other El Niño events, coastal Kelvin waves have been observed to propagate along the coast of North America as far as the Aleutian Islands[25]. c, Model SSH deviation 9 months after the time of *a*. The high SSH along the North American continent begins to peel away from the coast as a westward-propagating Rossby wave. (The colour bar at the bottom of the Figure applies to *a*, *b* and c).

Concurrent with the recent abundance of satellite data is a revolution in our ability to numerically model the dynamical processes in the oceans. From a numerical model simulation[8], we use results which cover the 12 years from 1981 to 1993. The model simulation and observational data provide independent results. This synergy is very important because results from one source alone may be inconclusive due to errors or assumptions made. SSH changes in the model simulation (Fig. 1*c*) indicate an anomaly from Japan to Alaska similar to that of the altimeter data. This suggests that the events that give rise to this ridge are realistically simulated in the model. The decadal simulation provides a unique, continuous, high-resolution data set which is used to identify the sequence of events which generate the observed trans-Pacific ridge. An animation of the model SSH variations from 1981 to 1993 clearly reveals that these events began in 1982 as a result of the El Niño.

The 1982–83 El Niño was initiated by the relaxation and subsequent reversal of easterly winds over the western and mid-Pacific[9], which generated an eastward-propagating equatorial Kelvin wave. (A Kelvin wave is a special class of shallow-water waves which occurs along the equator or along coastlines[10].) The Kelvin wave was reflected from the American continents as a westward-propagating Rossby wave, a class of waves that depend on the sphericity and rotation of the Earth (Figs 2 and 3). The Rossby wave reflection process and initial westward propagation in response to the 1982–83 El Niño have been simu-

lated by other ocean models[11]. The subsequent propagation of the El Niño-generated Rossby wave across the entire North Pacific is summarized in Fig. 3.

The implications of these results are far-reaching and unanticipated. Up to now, propagation of a Rossby wave across the Pacific Ocean at these high latitudes has never been demonstrated. Comparison of the Geosat altimeter data at 30° N with model results verifies the trans-basin journey of the wave (Fig. 4). Rossby waves, observed at the coast of the American continents[12,13], were not expected to propagate an appreciable distance into the basin as coherent structures. The energy of the wave was expected to cascade to smaller scales (that is, the wave would dissipate into eddies) and not to propagate as far as Hawaii at this latitude. However, our observations and simulations indicate that the Rossby wave not only remained intact as far as Hawaii, but continued across the basin and is coherent

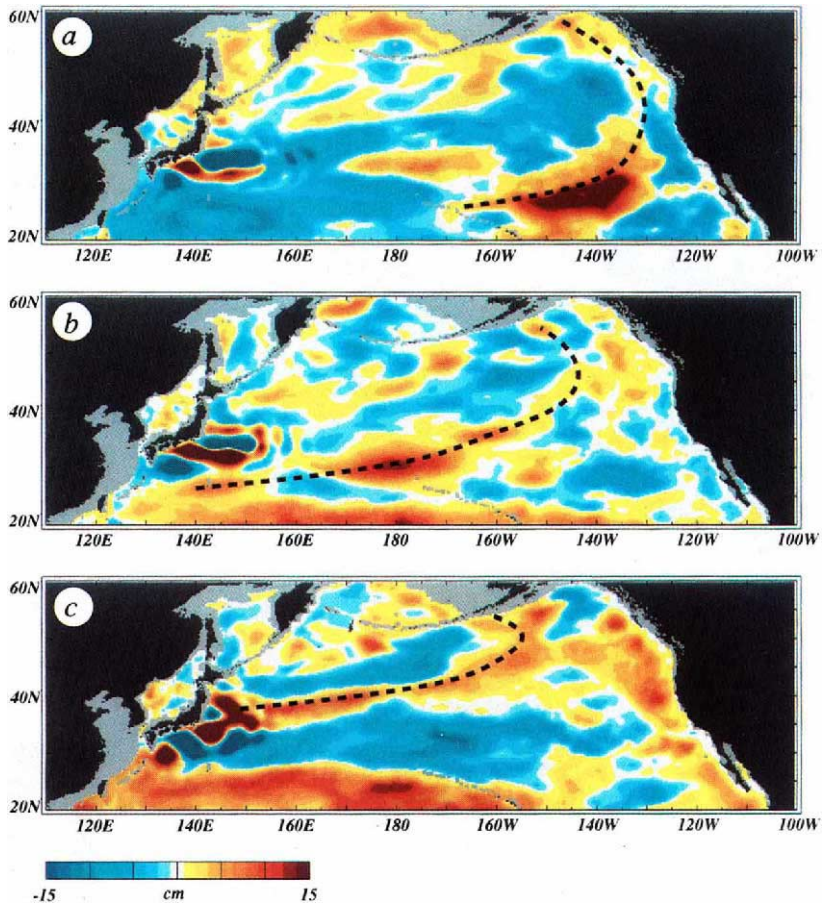

FIG. 3 Model SSH is averaged over 1 year to reduce short-timescale variability (*a*, over March 1984 to February 1985; *b*, over May 1987 to April 1988; *c*, over April 1992 to March 1993), and the 11-year model mean SSH is subtracted. The Rossby wave SSH ridge is indicated by the dashed line. *a*, Model SSH deviation 2 years after the 1982–83 El Niño. The Rossby wave shown in Fig. 2c has propagated away from the shore. *b*, Model SSH deviation 5 years after the 1982–83 El Niño. The Rossby wave extends from Taiwan to the Gulf of Alaska. The decrease in Rossby-wave phase speed with increasing latitude causes bending of the wave front[12]. At the northern end, the wave propagates very slowly. Five years after the 1982–83 El Niño, high SSH is still observed near the northwest coast of North America. At the same time, the southern end of the wave has already swept past the Hawaiian Islands. *c*, Model SSH deviation 10 years after the 1982–83 El Niño. The Rossby wave has moved to a position extending from Japan to Alaska. (The colour bar at the bottom of the Figure applies to *a*, *b* and *c*.)

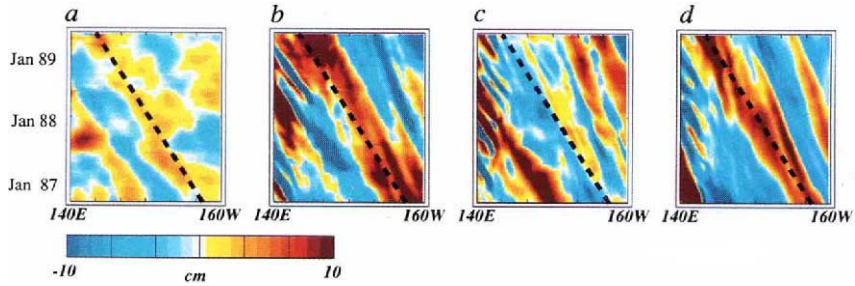

FIG. 4 SSH variations along 30° N from Japan to north of Hawaii; *a*, from the Geosat altimeter mission and *b*, from the model over November 1986 to July 1989. The mean SSH from 140° E to 160° W at each point in time has been removed to reduce the effects of the annual steric anomaly due to seasonal heating and cooling of the ocean surface. The dashed line indicates the propagation of the Rossby wave generated by the 1982–83 El Niño across the Pacific Ocean. The propagation speed at 30° N for the wave is 4.9 cm s^{-1}, which is very close to the theoretical value of ~5 cm s^{-1} for a non-dispersive, internal Rossby wave. *c*, In this simulation the wind anomalies which cause the equatorial Kelvin wave associated with the 1982–83 El Niño are removed. The equatorial Kelvin wave and subsequent Rossby wave never occur. *d*, In this simulation, the predictivepower of the model is demonstrated by forcing with observed winds only over the period 1981–84 and winds with only an annual variation afterwards. The equatorial Kelvin wave results, and the Rossby-wave chain of events occurs. This phenomena is therefore predictable on decadal scales. (The colour bar at the bottom of the Figure applies to *a*, *b* and *c*).

well over a decade later. The Rossby wave generated by the 1982–83 El Niño exists today in the northwest corner of the Pacific Ocean.

Additional evidence for this wave is given by a positive dynamic height anomaly observed in hydrographic data south of Japan at 137° E (ref. 14). This anomaly moves from 18° N in 1984 to almost 30° N in 1989, which agrees well with the movement of the Rossby wave in Figs 3 and 4. Thus, the Rossby wave propagating from North America to the Kuroshio Extension is observed in both the model and the ocean. Two additional ocean model simulations were performed to help isolate the decadal effects of the 1982–83 El Niño. One simulation was initialized in 1984 after the El Niño, and shows the absence of the El Niño-generated Rossby wave at 30° N (Fig. 4*c*). The other simulation starts in 1981, includes the 1982–83 El Niño, but the wind forcing reverts to an average annual forcing in 1984 to exclude subsequent wind-forced anomalies. It shows the Rossby wave (Fig. 4*d*), and because no knowledge of actual events in the atmosphere after 1984 was used, it demonstrates the potential for decadal predictions of El Niño-generated Rossby waves and their effects.

In the model, the Rossby wave produces a significant geostrophic velocity anomaly of $\sim 10\ \mathrm{cm\ s^{-1}}$ in the upper ocean as the wave passes through the Kuroshio Extension in 1991. The geostrophic flow induced by the trailing edge of the Rossby wave reduces the flow of the Kuroshio Extension along 35° N. The leading edge of the Rossby wave induces an eastward velocity perturbation near 40° N. The result is a re-routing of a portion of the Kuroshio Extension transport to ~40° N during 1991 and subsequent years. During 1991 the largest SST anomalies are found north of the Kuroshio Extension coincident with the maximum Rossby wave effects on the current. These anomalies reach a peak of >1 °C above mean values observed at other times. After the Rossby wave propagates to the northwest, the geostrophic perturbations on the Kuroshio Extension abate; the extension returns to its normally observed latitude, and the anomalous SSTs begin to disappear.

Corroboration of these events is provided by satellite infrared frontal analyses (J. Szezechowski, unpublished results), which indicate a northward displacement of the Kuroshio Extension in 1990–91 and a southward displacement from 1991 to 1993. In 1992–93, the Rossby wave forms a ridge of high SSH from Japan to Alaska (Fig. 3*c*). The results presented here indicate that the events giving rise to the trans-Pacific SSH ridge and SST anomaly in 1991–92 originated with the 1982–83 El Niño. Thus the oceanographic effects of a major El Niño have extratropical and decadal components.

Climatological effects associated with warm, tropical SST anomalies during major El Niño events are well-documented[15]. Surprisingly, the SST anomalies that we observe at much higher latitudes across the North Pacific are of the same amplitude and temporal-spatial extent as those observed in the tropics during major El Niño events. At higher latitudes, significant statistical relationships between SST anomalies in the Pacific Ocean and weather patterns over the North American continent have been found[16]. Thus it is possible that the 1982–83 El Niño still has important effects on the climate in 1993. Stated succinctly, the 1982–83 El Niño is not over: its effects have moved from South America to the northwest across the Pacific basin. This Rossby wave should continue to propagate across the far northwest corner of the North Pacific basin for at least another decade, and continue to affect the circulation of the North Pacific.

The deterministic nature of the processes that we report indicates that the ocean is not wholly chaotic and unpredictable, even over basin and decadal scales. Relatively simple planetary wave dynamics, the numerical models that include them, and global satellite data sets provide the necessary tools for long-term oceanic predictions (Fig. 4). Finally, we note that these long-timescale events imply that attempts to determine the climatological or average state of the oceans (a major component of Earth's climate) will require monitoring of the ocean circulation over decadal timescales. This is indeed a major task which will require synergistic use of numerical ocean models and continuous satellite monitoring for a complete understanding. □

Received 17 January; accepted 9 June 1994.

1. Cane, M. A. *Science* **16,** 1189–1194 (1983).
2. Barber, R. T. & Chavez, F. P. *Science* **16,** 1203–1208 (1983).
3. Barber, R. T. & Chavez, F. P. *Nature* **319,** 279–285 (1983).
4. Rasmusson, E. M. & Wallace, J. M. *Science* **16,** 1195–1202 (1983).
5. Folland, C. K. & Owen, J. A. in *Rep. of a Workshop at the European Centre for Medium-Range Weather Forcasting* 102–114 (Publ. No. 254, WMO, Geneva, Switzerland, 1988).
6. Born, G. H., Mitchell, J. L. & Heyler, G. A. *J. astr. Sci.* **35,** 119–134 (1987).
7. Reynolds, R. W. & Marsico, D. C. *J. Clim.* **6,** 768–774 (1993).
8. Hurlburt, H. E., Wallcraft, A. J., Sirkes, Z. & Metzger, E. J. *Oceanography* **5,** 9–18 (1992).
9. Wyrtki, K. *J. phys. Oceanogr.* **5,** 572–584 (1975).
10. Gill, A. E. *Atmosphere-Ocean Dynamics* (Academic, Cambridge, UK, 1982).
11. Johnson, M. A. & O'Brien, J. J. *J. geophys. Res.* **95,** 7155–7166 (1990).
12. White, W. B. & Saur, J. F. T. *J. phys. Oceanogr.* **13,** 531–544 (1983).
13. Jacobs, G. A., Emery, W. J. & Born, G. H. *J. phys. Oceanogr.* **23,** 1155–1175 (1991).
14. Qiu, B. & Joyce, T. M. *J. phys. Oceanogr.* **9,** 1062–1079 (1992).
15. Glantz, M. H., Katz, R. W. & Nicholls, N. *Teleconnections Linking Worldwide Climate Anomalies* (Cambridge Univ. Press, 1991).
16. Barnett, T. P. & Preisendorfer, R. *Mon. Weath. Rev.* **115,** 1825–1850 (1987).
17. Teague, W. J., Carron, M. J. & Hogan, P. J. *J. geophys. Res.* **95,** 7167–7183 (1990).
18. Hurlburt, H. E. & Thompson, J. D. *J. phys. Oceanogr.* **10,** 1611–1651 (1980).
19. Wallcraft, A. J. *NOARL Report No. 35* (Naval Research Lab, Stennis Space Center, 1991).
20. Metzger, E. J., Hurlburt, H. E., Kindle, J. C., Sirkes, Z. & Pringle, J. M. *Mar. Technol. Soc. J.* **26,** 23–32 (1992).
21. Hellerman, S. & Rosenstein, M. *J. phys. Oceanogr.* **13,** 1093–1104 (1983).
22. McCreary, J. *J. phys. Oceanogr.* **6,** 632–645 (1976).
23. Hurlburt, H. E., Kindle, J. C. & O'Brien, J. J. *J. phys. Oceanogr.* **6,** 621–631 (1976).
24. Kindle, J. C. & Phoebus, P. A. *J. Geophys. Res.* (in the press).
25. Chelton, D. B. & Davis, R. E. *J. phys. Oceanogr.* **12,** 757–784 (1982).

ACKNOWLEDGEMENTS. This work was supported by the US Office of Naval Research and the US Advanced Research Projects Agency.

A unique multitoothed ornithomimosaur dinosaur from the Lower Cretaceous of Spain

Bernardino P. Pérez-Moreno*, José Luis Sanz, Angela D. Buscalloni, José J. Moratalla, Francisco Ortega & Diego Rasskin-Gutman

Unidad de Paleontología, Departamento de Biología, Facultad de Ciencias, Universidad Autonóma de Madrid, 28049-Madrid, Spain

THE Lower Cretaceous lithographic limestones from Las Hoyas (province of Cuenca, Spain) have yielded important vertebrate fossil remains. We report here a new specimen, the first ornithomimosaur theropod found in Europe. *Pelecanimimus polyodon* gen. et sp. nov., has some striking elements preserved, such as the hyoid, sternum and integumentary impressions. The fossil has revealed other unexpected features, including a derived hand in an ancient ornithomimosaur, and a large number of teeth (over 200) with a distinctive morphology. This specimen suggests an alternative evolutionary process towards the toothless condition in Ornithomimosauria, which could be explained by an exaptation. *Pelecanimimus polyodon* stresses the relationship between Troodontidae and Ornithomimosauria.

The Las Hoyas fossil site is one of the most important conservative *lagerstätten* from the Lower Cretaceous of western Europe. It has yielded thousands of specimens including two of the most primitive birds ever found: *Iberomesornis romerali*[1,2] and *Concornis lacustris*[3]. A diversified flora and fauna from a lacustrine environment have also been discovered in these lithographic limestones[4]. Non-avian dinosaur remains have not previously been found in Las Hoyas limestones, although some sauropod and *Iguanodon* bones were discovered in equivalent strata of